The Eurasia Proceedings of Science, Technology, Engineering & Mathematics (EPSTEM)
ISSN: 2602-3199

The Eurasia Proceedings of Science, Technology, Engineering and Mathematics (EPSTEM), 2025

Volume 37, Pages 1054-1067

ICEAT 2025: International Conference on Engineering and Advanced Technology

Bond Performance of Concrete-To-HPC Interface for Different Surface Profiles Using Slant and Bi-Surface Shear Test

Bushra Hussein Al-Aboudi
University of Al-Qadisiyah

Haider M. Al-Jelawy
University of Al-Qadisiyah

Abstract: Concrete structures are usually used in all construction fields. However, it is exposed to cracking and corrosion over time, especially when exposed to harsh conditions. This requires continuous repairs to ensure the structure's functionality, durability, and safety. High-Performance Concrete (HPC), is one of the best concretes which used for repairing. This study was conducted to assess the influence of different surfaces of normal concrete (NC) and the use of bonding agent on the adhesion strength of High-Performance Concrete (HPC). The trial work was based on a set of composite samples, where the substrate was made of (NC) and the cover layer was made of (HPC). A commercial bonding material (epoxy resin) was used to bond the NC with a smooth surface to the HPC layers of concrete. Three substrate surfaces were considered: a smooth surface, a smooth surface coated with epoxy, and a rough surface. The adhesion performance was evaluated through two tests: the slant bond test and the bi-surface test after 28 days of curing. DIC (digital technique correlation) was applied to notice the process of failure in specimens. The preliminary results showed that the bonding between the two types of concrete was very good. The best bonding strength was NC with the rough surface bonded by HPC, followed by the smooth surface-epoxy, and then the smooth surface by mean (5.83, 4.73, 3.92) respectively for the bi-surface test, and by mean (6.89, 5.68, 4.71) respectively for the slant bond test. However, further studies are needed to test more types of surfaces and different conditions.

Keywords: Bi-surface test, Different surfaces, Slant bond test, Epoxy-resin

Introduction

Concrete structures are exposed to many factors that cause corrosion and cracks during their service life, such as load bearing and the environment (Feng et al., 2020). Maintaining these structures helps to benefit from their required function for a longer period. The rapid increase in infrastructure deterioration has led to asignificant attention in the bond between the current concrete substrate with the repair materials. Good adhesion between old concrete and new concrete is one of the most effective methods of repairing structures (Tu, Chen, & Hwang 2006). The use of concrete bonding has expanded and has gone beyond being a mere repair or completion of work in progress that has been stopped for various reasons. Thus, the repair layer or bonding layer does not have to be an external layer. For instance, it can be an alternative solution to expansion joints between adjacent bridge panels, because expansion joints are most likely to cause damage (Kinaine & Al-Jelawy 2023; Al-Jelawy & Kinaine, 2024; Al-Jelawy et al. 2025). These connections are made of UHPC concrete which has proven its efficiency (Al-Jelawy et al. 2024; Alzamily et al. 2025). HPC is defined as concrete that is stronger and durable than NC(Sohail et al. 2018). It achieves (70- 80MPa) compressive strength (C.S) for 28 days. It contains a big quantity of silica fume, cement, superplasticizer, high-quality fine aggregate and a low water/cement ratio less than 0.35 to gain high density, low permeability, and high strength (Büyüköztürk & Lau 2002). Although high cost compared with NC, using HPC has been created to be low cost for the high and complex buildings, bridges, columns and structures that are exposed to many types of sulfates, chlorides and corrosion. One of the best repair layers, which consists of cement, fine sand, superplasticizers, silica fume and

steel fibers. These materials work together to enhance the high strength and durability of concrete, thus preventing the entry of salts and other obstacles.(Benjamin A. 2006). Researchers have taken care of the bond strength between HPC and NC. The results explained that many parameters influenced on bond strength of HPC-NSC, such as the treatment of the interface surface, HPC age and curing method, NSC compressive strength, and the moisture conditions of the interface(Farouk & Jinsong 2022). However, adhesion in the aggregate interlock, interface, friction, and the factors that time-dependent significantly influence the bond strength, in addition to the test method used. which again is influenced by other variables such as Adhesion to the interface influenced by bonding agent, roughness degree of interface surface, material compaction and specimen age. Otherwise, aggregate interlock and friction at the interface depend on size and shape aggregate and surface preparation.

The chosen test method is determining the size, geometry of specimen and the bonding method, so several standard tests have been advanced for specific applications. For instance, the slant bond is used to estimate the bond strength of epoxy bonding agents, resinous materials, under compression and shear (Momayez et al. 2005). Sun et al. (2023) studied the bonding strength of prism specimens (100 × 100 × 300 mm) by slant test. Different roughness levels (unroughened, brushed, and sliced) were applied to the bonding surfaces between two layers of concrete of the same type and mix proportion, but with two different setting retarder (0% and 1%) for the old concrete, surface roughness, and different curing times (8, 16, 24, and 72 hours). New concrete was poured as the old concrete began to set. Compressive strength, failure modes, and displacement were measured to comput the bonding strength of the specimens. It was concluded that the specimens with the retarder showed adequate bond strength 16 hours after the previous pouring than the specimens without the setting retarder, because the addition of the retarder increased the setting time. The specimens with the brushed surface had stronger bonding than the other surfaces. Consoli et al.(2013) studied the bond between UHPC and normal strength concrete (NSC) with varying concrete substrate roughness, exposure to freeze-thaw cycles, bond age and wet conditions of the concrete substrate. A combination of split tensile test, slant shear test at different interface angles and bond tensile strength measurements were performed, using a pull-out test. The study concluded that when exposed to freeze-thaw cycles, the bonding performance develops with the presence of saturated concrete. This may be because UHPC is a concrete with a low w/c, so there is a much greater amount of non-hydrous particles. The bonding performance at older ages gives outstanding outcomes under tensile stress, without focusing on the roughness of the substrate or its exposure to freeze-thaw cycles. The bonding and high adhesion strength at 8 days are better than that of the concrete substrate. The degree of roughness of the concrete substrate (friction) was not a decisive factor for good bonding strength. Valikhani et al. (2020) investigated the bond strength between UHPC and NC. Specimens were tested under a bi-surface shear test using different surfaces (smooth, sandblasted (with or without a mechanical connector made of steel reinforcement), and a smooth surface coated with epoxy). Two non-contact testing methods were used, including digital image processing and terrestrial laser scanning to screen the substrate interface roughness and correlate the degree of roughness with the bond strength between two materials. The outcomes indicated that the rough surface, with or without the presence of mechanical connectors, transported the failure to the concrete substrate, due to the higher bond strength between the two materials compared to other surfaces. It was concluded that adding a bonding agent to the sandblasted surface decreased bond strength due to reduced interlocking between the two materials.

The results for the smooth surface, with or without epoxy, were similar because they relied on the high chemical bond between the two layers. Sun et al. (2023) investigated the epoxy bonding agents on interfacial (NC) to (UHPC) behavior by both molecular dynamics simulation (MDS) and experimentation methods. The bonding strength was tested by slant shear and splitting tensile tests. They applied a quantitative analysis of backscattered electron images and X-ray diffraction to estimate the microstructure of the overlay transition zone between NC-UHPC. MDS was joined with the macro experiments to explore the bonding mechanism between calcium silicate hydrate (C-S-H) and three bonding agents under moisture conditions: E-51 epoxy resin, waterborne epoxy resin (WEP) and waterborne epoxy resin modified by a silane-based coupling agent (WEP-SCA). He found that WEP can improve the bonding property of a damaged NC substrate, while this decreases with a smooth NC substrate. E51 harms bonding property. The NC substrate moisture has no significant influence on the microstructure of OTZ and bonding strength. At the molecular scale, the bond strength growth between C-S-H and epoxy by the adhesive is very slight, while the hardness can be improved to some extent. The Load-Slip method has been adopted in many studies to evaluate the type and amount of slip displacement in the bonding zone between two types of concrete(Liu et al. 2020; Zhang et al., 2020; Hu et al., 2020) used a different method to roughen the surface by creating rows of rectangular grooves on surface concrete substrate. Two groove depths, 3 and 6 mm, and two angles of inclination from the vertical, 30 and 40 degrees, were designed. slant bond tests were performed after 60 and 120 days, and the samples were exposed to dynamic and quasi-static loads. It was concluded that the probability of bond failure is greater for specimens at a 30° inclination angle than for specimens at a 40° inclination angle, regardless of whether the specimens are subjected to quasi-static or dynamic loads. The slant bond strength of the specimens increases when the inclination angle changes from 30° to 40°. Furthermore, surface roughness has a negligible effect on slant shear behavior, and the effect of age can be ignored. Although bond tests have been developed, there is no actual deal for evaluating the bond strength under different surfaces in buildings. So this research aims to monitor the bonding force with different surface roughnesses,

which were prepared in a simplified way that simulates reality without the complications that were carried out in the previously mentioned research.

Materials and Methods

Materials

High-Performance Concrete

HPC is a high-performance concrete with high uniformity that cannot be succeeded using conventional ingredients, mixing and pouring methods, or normal curing. It is characterized by high strength, low porosity, heat resistance, and high flowability. These properties combine to provide improved performance in harsh environments (such as high relative humidity, high temperatures, sulfate and chloride reactions, and carbonation). According to the American Concrete Institute (ACI) Committee 363, its design strength is 55 MPa or greater (Sohail et al. 2018).

The general formulation of proprietary HPC consists of Portland cement, silica fume, steel fibers, superplasticizer and quartz flour. HPC is also used in new structures for beam shells, column HPC shells and closure joints between pre-fabricated bridge deck elements (Aïtcin 2003). The use of adhesive bonding agents has become increasingly popular because it offers greater surface adhesion and water resistance. Many factors control the effectiveness of the bonding agent, such as viscosity, thermal expansion, compatibility with concrete components, shrinkage, its physical and chemical properties, surface condition, environmental factors, and the method of application (Daneshvar, Behnood, & Robisson 2022).

In this study, HPC is used equally as a repair layer to NC substrates. The Components of the mixes of HPC and NC are listed in Table 1. The C.S was measured established on ASTM C109(ASTM 2020). The Portland cement III high strength, Straight steel fiber (12mm and l/d =65) 1%, fine aggregate with maxi- mum size (600 μm) which is ready by sieving sand to obtain required grading, commercially available high-range water reducer polycarboxylate polymer (3rd Generation) 1%, gray silica fume with (specific gravity 2.4) were used.

Table 1. Components of the mixes of UHPC and NC

Materials	NC(Kg/m³)	UHPC(Kg/m³)
Cement	455.56	1000
Sand	660.13	-
Fine sand	-	1000
Coarse agg.	1024	-
Silica fume	-	100
superplasticizer	-	30
Steel fiber	-	78
water	205	280
Comp. strength (MPa)	22	74

Normal Concrete

Mixture of NC is listed in Table (1) with a (100 mm) slumping**.** Sampling and compacting were supported by the (ASTM C31)(ASTM C192/C192M 2016). Portland cement is the same as in HPC, the maximum size of fine aggregate particles is (5μm), and the grading size of coarse aggregate is (19 -5 mm). The aggregate is cleaned from clay, then drying the gravel to obtain a saturated surface dry aggregate.

Experimental Methods

Preparing the Models

Nine cube samples were prepared (150*150*150 mm) for the bi-surface test and three cubes for the compressive strength of NC. Nine-cylinder samples (75*150mm) for the slant bond test and three cubes (50*50*50 mm) for the compressive strength of HPC. The cylinders were fabricated locally. Mold was treated with oil, and NC was placed in two-thirds of the cube volume and half of the cylinder. A wooden piece was made with dimensions (14*14*5) to

ensure the thickness of the repair layer. After 7 days, the molds were completed with the UHPC layer Fig.1. After two days, the workforms were demolded and the samples were located inside basins at a moderate heat of 60 ℃ for 28 days.

(a)

(b)

Figure 1. The pouring process for (a) cylinder, (b) cube

Preparing the Surfaces

Roughness is an essential factor in bonding between substrate and new concrete and one of the most significant matters that should be attended to in repair and rehabilitation for concrete structures, as ACI 546 (Diab, Abd Elmoaty, & Tag Eldin 2017). Three degrees of surfaces Fig.2 were primed before HPC placement: smooth L.S., rough L.R. and a smooth surface coated by epoxy resin L.E. by brush. Some molds were demolded to treat and smooth their surfaces as required, while the rough surfaces were left as cast without smoothing. The presence of coarse aggregate is visible on the concrete surface. Half of the soft surfaces were coated with epoxy resin

(a) (b) (c)

Figure 2. Surface preparation (a) smooth L.S, (b) epoxy resin L.E, (c) rough L.R

Bonding Agent

The bonding agent was a saleable epoxy resin-based (Quickmast 108) bond coat in two components, Quickmast 108 base, and Quickmast 108 hardener Fig.3 (a,b). The epoxy used is applied on dry and wet surfaces. To apply the epoxy

on concrete substrates the epoxy components were mixed for at least 3 minutes, until getting a uniform color Fig.3(c). Surface cleanliness has been confirmed before the epoxy is applied at 23 ± 2 °C, humidity of 50 ± 5%. It is applied with a thickness of 2-3mm left until it becomes tacky before the HPC layer is placed. Slant Shear molds are prepared at an inclined vertical angle (30◦) according to ASTM C882/C882M(ASTM 2010).

(a) (b) (c)

Figure 3. Epoxy resin (a) Hardener, (b) Base, (c) mixing (a) & (b)

Test Method

DIC (Digital Image Correlation)

For both tests during the process of load, digital image correlation (DIC), a visual non-destructive optical technique was adopted to determine strain field and the displacement distribution on the surface specimens in addition to monitor the failure (Fig.4a). One of the specimen surfaces containing the connection between the two concretes was painted and then dotted with black. The Nikon camera was working to photograph the loading stage. A photo was taken every second. The camera resolution is 24.1 Mica pixels. GOM Correlate 2019 was used to investigate the recorded data and obtain the required results from successive images taken. As shown in (Fig.4b), a dial gauge was mounted on tester panel surface to determine the relative displacement between the NC and HPC.

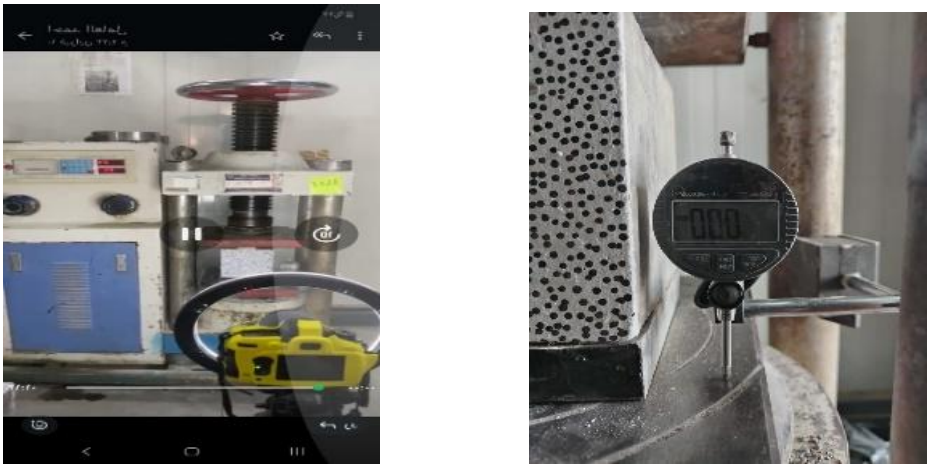

(a) (b)

Figure 4. (a) DIC measurement system (b) dial gauge

Bond Strength

The results values of the bond strength of NC-HPC specimens were calculated using bi-surface test and slant test. For the bi-surface test, the specimens were overloaded on three points regularly putting three steel plates (15*5*2 cm) as shown in Fig. 5b. Those values characterize the average bond strength. For the bi-surface test, the bonding strength has been obtained by dividing the load failure by the bonded surface area. According to the slant bond test, the specimen was subjected to vertical compressive load throughout the machine's loading plate, as illustrated in Fig. 5a. The load was applied continuously and stopped when the recorded load decreased suddenly because of the specimen's failure. The bi-surface bond strength is computed as the ratio of the applied failure load to the bonded surface area

according to Equation (1) (Al-Rubaye, Yousef, & Muteb 2020) .

$$fs = \frac{F}{A} \quad (1)$$

fs: bond strength (MPa), F: failure force (N), A: bonded surface area (mm²).

(a) (b)

Figure 5. (a) slant bond test (b) bi-surface shear test the bonded area for slant bond test is calculated as an ellipse.

$$A = 0.7854ab \quad (2) \text{ (ASTM 2010)}$$

Results and Discussion

The specimens were named to distinguish them throughout the work and the test. L.S. represents the smooth surface, L.E. represents the epoxy resin surface and L.R. symbolizes the rough surface. Figure 6. The interface perspective of the three samples with differing surfaces following the slant shear test is illustrated. The bond of L.E. is defined by the epoxy layer affixed to HPC, with a thin layer of NC eliminated across the majority of the bond region.

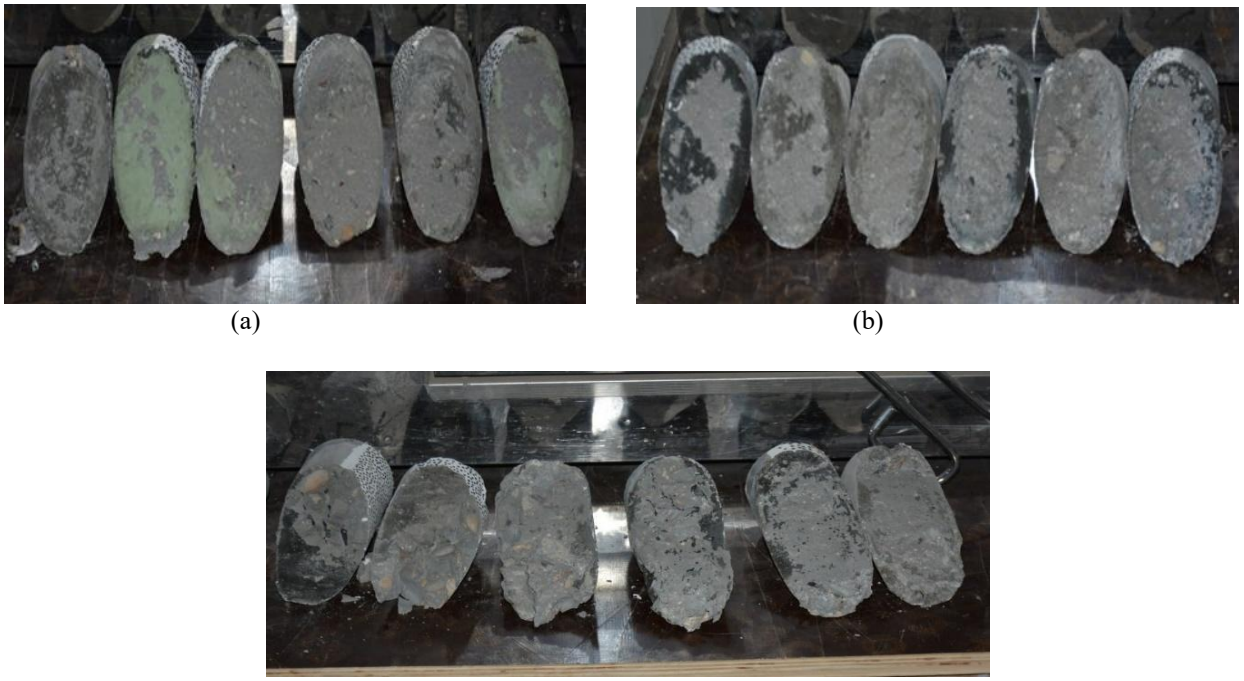

(a) (b)

(c)

Figure 6. Slant shear test (a) epoxy resin (b) smooth surface (c) rough surface at 28 days.

L.S. was mostly pure with a little layer removed with the bond in some specimens, while in L.R., the failure was in part of the bond with some NC cracking. Figure 7 shows the interface perspective of three samples with different surfaces after testing with a bi-surface test. The failure was in the adhesion NC layer with epoxy and tinny parts of the concrete. The failure in L.S. was pure, while the failure in the NC layer for L.R. and there were little cracks.

(a)

(b)

(c)

Figure 7. Bi-surface test (a) epoxy resin (b) smooth surface (c) rough surface at 28 days

After failure, the bond failure shapes were classified into three types: (A) was pure bonding failure between the two layers, (B) was bonding failure with a small amount of the NC layer, and (C) was cracking in the NC layer and bonding failure. In all cases, there were no cracks in the HPC layer due to high-strength performance. It is evident from tables (2,3) that the highest bonding performance was recorded in L.R, ranging from 5.49 to 6.17 MPa, with a mean of 5.83. The bond strengths were increased in L.R. in both tests due to an increase in adhesion force with increasing interface roughness. Also, another factor that helps increase bonding strength of L.R. is the presence of aggregates on the concrete surface, which increases the surface area exposed to bonding, which is lacking in L.S. (B. Zhang et al. 2024).

The bond strength in L.R. is upper than surface coating with the L.S. and L.E. (150%, 121%), respectively. This result is according to (Valikhani et al. 2020). Adding epoxy resin increases bond strength by an average of (3.92 to 4.73) compared with L.S. because of its strong adhesive property with a thin layer of NC (Santos, Santos, & Dias-Da-Costa 2012), mean of 4.99. The value of the variation coefficient in bi-surface test is around (4.12 – 5.88) %.

Table 2. The bond strength, mean, the variation coefficient and failure mode for the bi-surface test of each set

Sample	Bond strength (MPa)	Mean	COV%	Mode failure
L.S.1	3.89	3.92	4.12	A
L.S.2	3.78			A
L.S.3	4.10			B
L.R.1	5.84	5.83	5.88	C
L.R.2	6.17			C
L.R.3	5.49			C
L.E.1	4.67	4.73	4.99	A
L.E.2	4.99			B
L.E.3	4.53			B

Table 3. Bond strength, mean, coefficient of variation and failure way for the slant bond test for the groups

Sample	Bond strength (MPa)	mean	COV%	Mode failure
L.S.1	4.99	4.71	6.64	B
L.S.2	4.76			A
L.S.3	4.37			B
L.R.1	6.78	6.89	1.58	C
L.R.2	6.99			B
L.R.3	6.91			C
L.E.1	5.50	5.68	2.89	B
L.E.2	5.73			B
L.E.3	5.81			C

The same behavior could be seen in the slant test, which is the largest result was obtained from the L.R. bond between (6.78-6.99 MPa), then (5.5-5.81 MPa) for L.E. finally (4.37-4.99 MPa) for L.S. The bond strength in L.R. is higher than in L.S. by an average of 46%. This result is according to Ding et al. (2022). Adding epoxy resin improves the bond, perhaps due to its chemical properties that enhance the adhesion (Diab et al., 2017). The value of the coefficient of variation in the slant bond test is around (1.58 – 6.64). In all cases, it is a low value, which indicates the uniformity of the outcomes with each other(Ding et al., 2022).

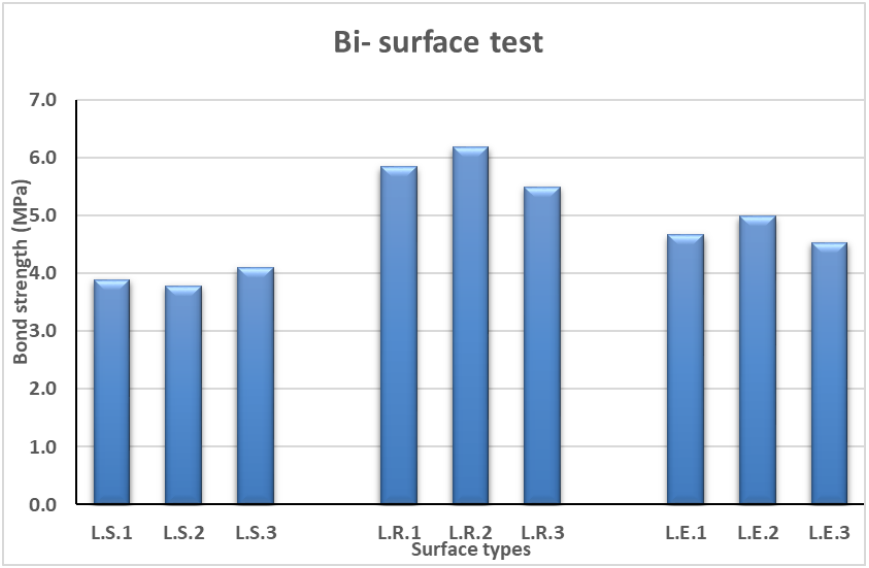

Figure 8. Bond strength for bi-surface test

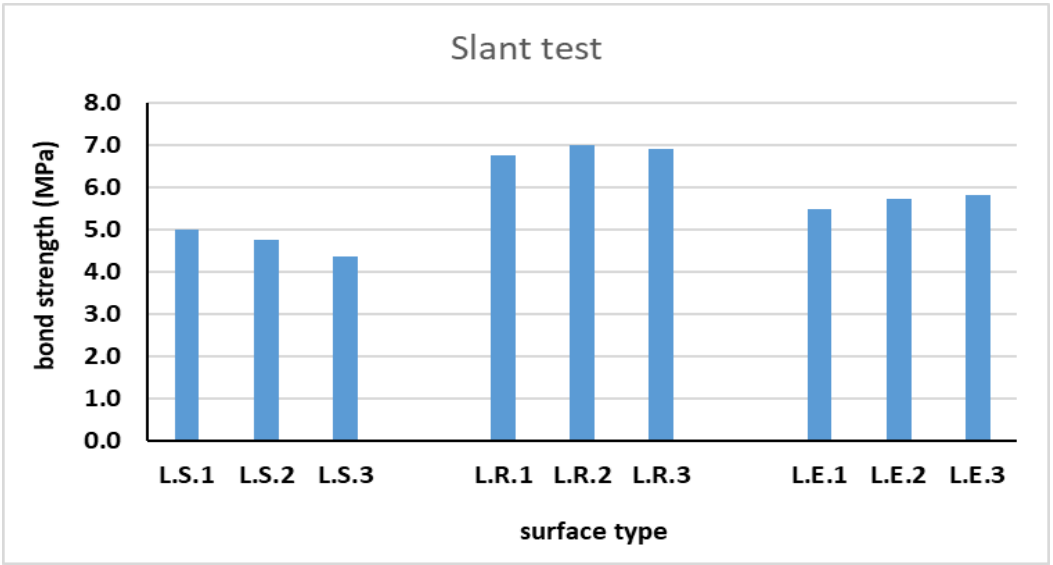

Figure 9. Bond strength for slant bond test

Fig. 10 compares the two kinds of tests for the different surfaces in bond strength evaluations. The bi-surface test values are generally less than the values of the slant bond test because the sample is exposed to shear stress in addition to compression force which cause a friction force, but in the bi-surface just pure shear stress(Pulkit et al., 2023).

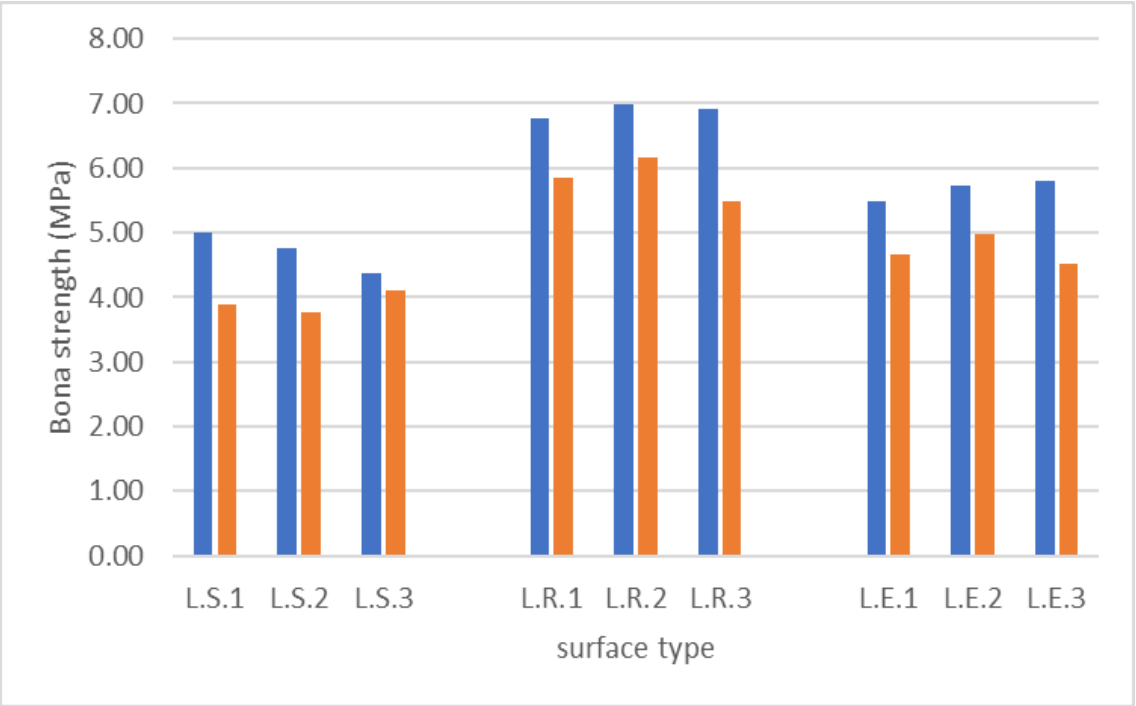

Figure 10. Comparison of the slant bond test by bi-surface test

Load Slip-Displacement

One dial gauge was used to calculate the average slip between the two layers in bi-surface test Fig (1b) and slant bond test. To draw the load-slip diagrams, the GOM Correlate 2019 was used to determine five points on one side of the connection corresponding to other points on the image of the model before slip and failure. The program then determined the slip value for these points in all stages of the load until failure. As for the cylindrical models, the points were determined in the middle only to achieve the correct enrichment of the flat surface. As previously declared, there are three failure phases, which are clearly shown in Figure 11.

The first phase (a) is failure which occurs suddenly only in the bonded region. The curve passes through a linear phase, where the slip value increases slightly with increasing load. This may be because of the difference in the Young's modulus of the bonded surfaces (Liu et al. 2023), and these values are usually negligible. The second phase (b) is failure exhibited a significant yield stage, the slip value increasing with a small increase in load to reach the failure stage without undergoing a strengthening stage.

The last phase (c) in addition to the linear phase (initial phase) and yield phase (final phase) mentioned above, there is a strengthening phase, resulting from the beginning and development of cracks in the NC, as well as interface cracks, with a minor gradient of the load-slip curvature despite the continuous increase in load. The specimens continue to resist a certain degree of damage. Finally, the curve enters the yield phase, until a sudden fracture occurs.

The average slip for the L.R, L.E and L.S surfaces for the bi-surface test is (0.256, 0.19, 0.179) mm respectively at the average load (131.69, 106.32, 84.76) KN respectively. The average slip for the L.R and L.E, L.S surfaces for the slant test are (0.035, 0.028, 0.013) mm respectively at the average load (59.95, 53.87, 41.58) KN respectively. This shows an enhancement in the strength and ductility of the NC-HPC interface when the bond agent is added or when the surface roughness increases compared to the smooth surface.

In Fig.11 (d,e,f), no linear path for the interface failure because of shear resistance and interlocking influence resulting from the total deformation from the compression and shear process and the deformation associated with compressive cracking of the NC section.

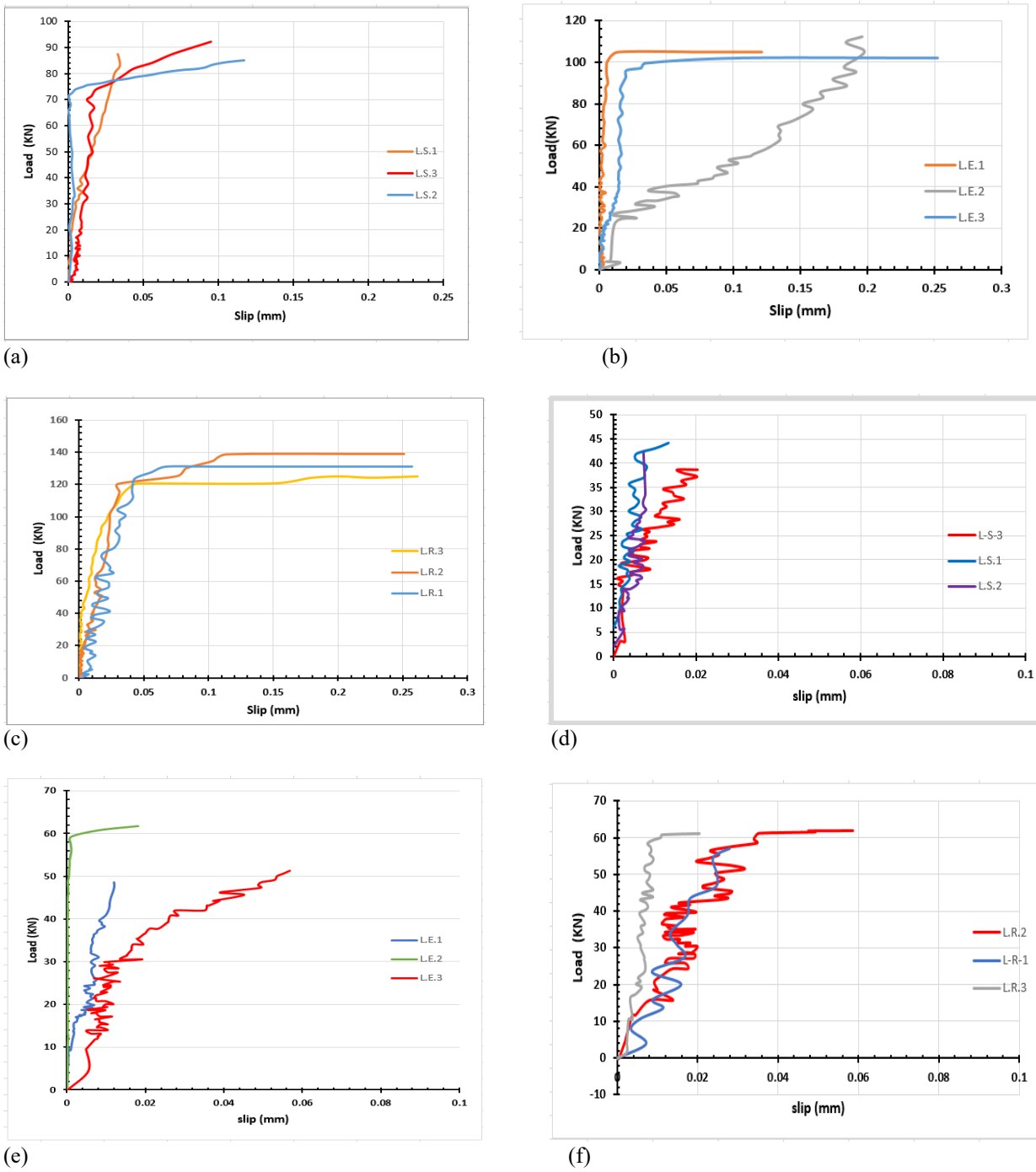

Figure 11. Relation of the load with interface slip, (a.b.c) special for bi-surface test, (d.e.f) special for slant bond test

Fig. 12 shows the major strain contours for the specimen of the bi-surface and the slant tests subjected to several loading stages, which were found by the DIC method. *P*u was the ultimate load of the bi-surface test specimen for each group. The strain propagation is shown in images in different load states, where it clearly appears with increasing applied load. In Fig. (a,b,c) strain contour for L.S., the sample was stable and the strain was spread in all the specimens directions at 50% of the applied load, increasing to 75% of the load, cracks began to concentrate in bonding area and separated at the ultimate load. In Fig. c, it is clear that the failure in the bond with thinner parts of NC sticking to the HPC.

Fig (d,e,f,g) showed the epoxy resin surface, which was an increased in bond strength to 87% of load with appearing the cracks in bond area and NC layer and more cracks. In Fig. g, the GOM Correlation software could not recognize the large part cracks, which were presented as a white area.

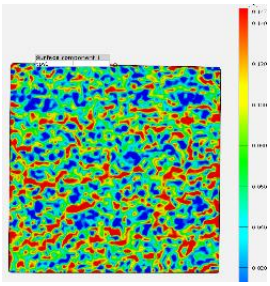

(a) 50 % Pu

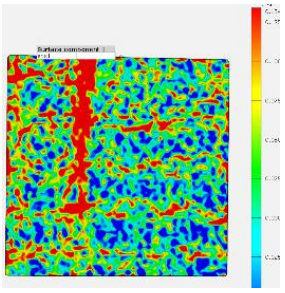

(b) 75 % Pu

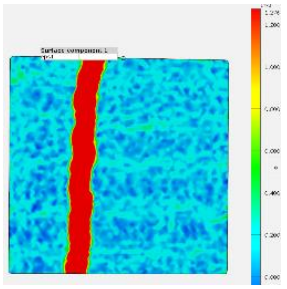

(c) 100 % Pu

strain for smooth surface

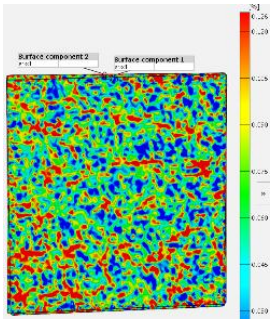

(d) 50 % Pu

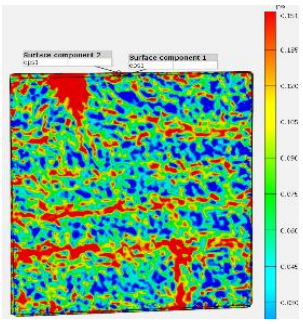

(e) 87% Pu

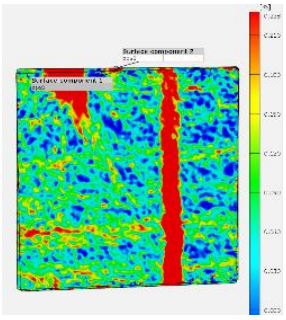

(f) 97 % Pu

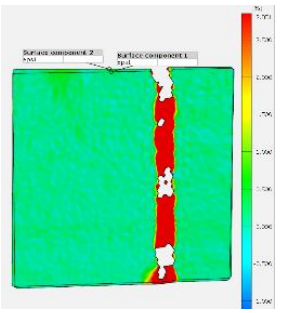

(g) 100 % Pu

strain contours for epoxy resin

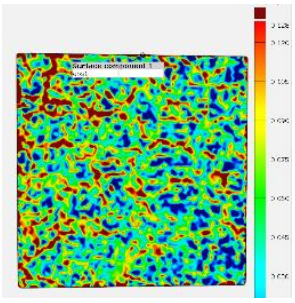

(h) 50 % Pu

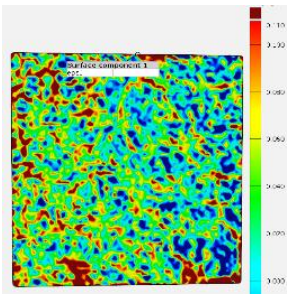

(i) 80% Pu

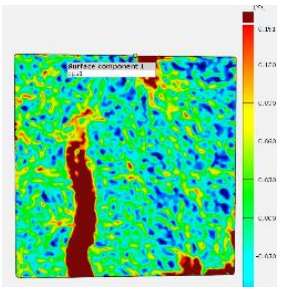

(j) 97 % Pu

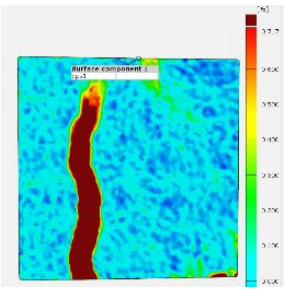

(k) 100 % Pu

strain counter for rough surface

Figure 12. Strain contours of bi-surface specimens

No cracks were observed on the bi-surface specimens in L.R. under the most loads state, while the strain was noted at the bond surface continuing from bottom up just to the mid interface at 97% Pu and two-thirds of the bond remains at maximum load. The strain contours are shown Fig. 13 for three different types of specimens analyzed in the study.

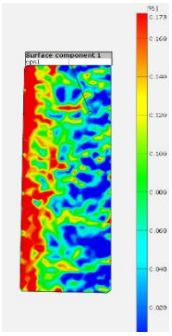

(a) 50% Pu

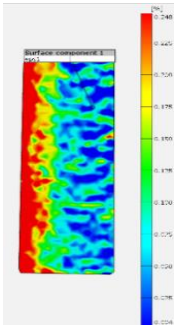

(b) 75% Pu

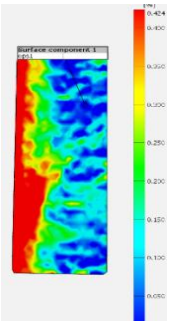

(c) 97% Pu

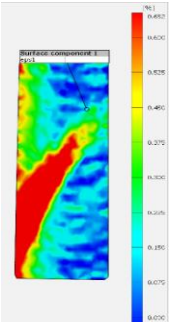

(d) 100% Pu

strain contours for L.S

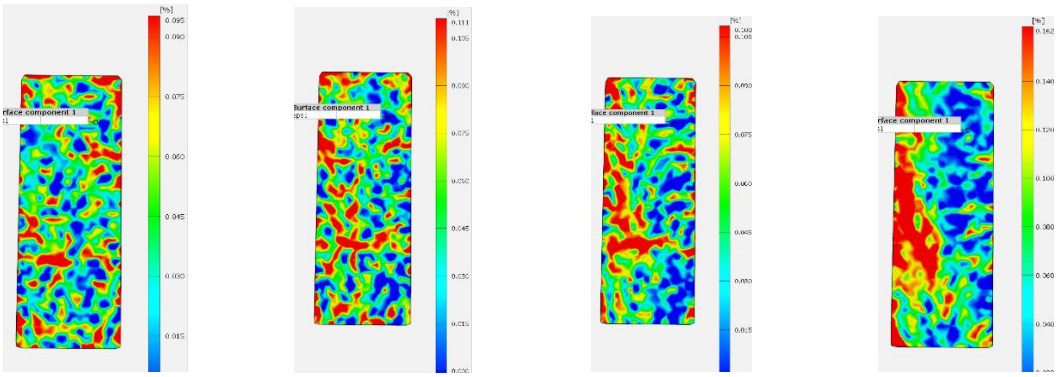

(e) 50% Pu (f) 75% Pu (g) 85% Pu (h) 100% Pu
strain contours for L.E

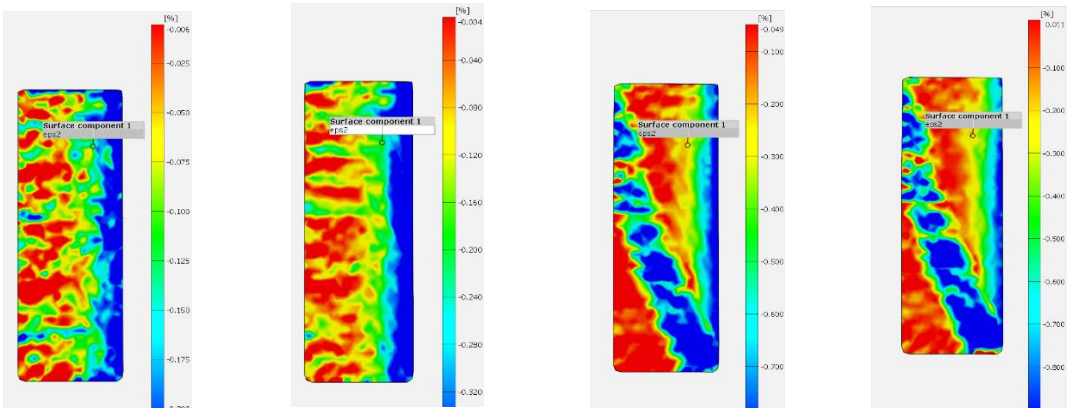

(i) 50% Pu (j) 75% Pu (k) 95% Pu (l) 100% Pu
strain contours for L.R

Figure 13. Strain contours of slant specimens

The figures (a) to (d) for L.S. the distribution of strain when the specimen is subjected to half of its maximum load capacity. It indicates relatively low and uniform strain levels and minimal deformation at this stage to 75% Pu. The distribution begins to appear more localized at (c) and is experiencing significant deformation approaching to full load. Sample L.E. showed the strengthening pattern which continued with a linear deformation until 50% followed by progression of it especially near the bond surface, until the end of the ultimate load where failure occurred in the bond and some small parts of the NC. For the rough surface sample, the continuation of the strain pattern from 95% of the applied give rise to the critical load is an indicator of the yield mode resulting from fracture of NC. The figures collectively demonstrate how strain propagates and concentrates within different regions of the specimens as the applied load increases, providing insights into the failure mechanisms and structural performance at various load levels. Generally, the smooth models showed easy and sudden debonding. L.E. showed irregular and heaving failure due to cracking concrete parts with failure of adhesion between the epoxy and the NC, while the failure in the case of L.R. was more evident in the NC in addition to the failure of the bond. The DIC test indicated that the bonding zone's presence did not result in strain separation. In fact, in some samples, the strain in the NC was clear and not yet concentrated in the joint. However, it may have affected the consistency of the strain field.

Conclusion

In this study, eighteen samples were examined to determine the bond NC to HPC using two different surfaces and the addition of a bonding agent. The results showed the failure phases and load-slip curve in bi-surface and slant bond tests. This investigation yields the following conclusions: Based on this and previous research, a smooth surface does not achieve good bonding, so the surface must be roughened before repair. Treating old concrete by roughening the surface serves as an efficient means for increasing the bond strength between the two concrete surfaces. Adding a bonding agent increased the adhesive strength, but the increase was small compared to the difference in results between the rough and smooth surfaces. The use of DIC examination enhances the interpretation and validation of numerical results.

Recommendations

This study was conducted on a small number of samples. Further research is needed with more samples to determine which types of binders increase the adhesion strength of the coating on smooth surfaces, as well as their application to rough surfaces with different thicknesses, in addition to determine the influence epoxy on surface roughness, and whether it increases or decreases the adhesion strength of the rough surface.

Declaration of Scientific Ethics

* The authors acknowledge that they bear full ethical and legal responsibility for this article published in EPSTEM.

Conflict of Interest

* The authors declare that they have no conflict of interest.

Funding

* This work and research were funded by the authors.

Acknowledgments or Comments

*This article was presented as an oral presentation at the International Conference on Engineering and Advanced Technology (ICEAT) held in Selangor, Malaysia, on July 23-24, 2025.

References

Aïtcin, P. C. (2003). The durability characteristics of high performance concrete: A review. *Cement and Concrete Composites*, *25*(4-5 SPEC), 409–420.

Al-Jelawy, H. M., Alzamily, A., & Jashami, H. (2024). Numerical modeling of link slab jointed rigid pavements. *In International Conference on Transportation and Development 2024* (pp. 381-391).

Al-Jelawy, H. M., & Kinaine, A. F. (2024, April). Development of jointless rigid pavement using ultra-high performance concrete link slab. *In AIP Conference Proceedings* (*Vol. 3079*, *No. 1*). AIP Publishing.

Al-Jelawy, H. M., Kinaine, A. F., Mousa, M. A., & Muhaisin, M. H. (2025). Advantages of using ultra-high-performance concrete (UHPC) link slabs as an alternative to dowel bar joints in rigid road surfaces. *Roads & Bridges/Drogi i Mosty*, *24*(1).

Al-Rubaye, M. M., Yousef, R. F., & Muteb, H. H. (2020). Experimental evaluation of bond strength performance between normal concrete substrate and different overlay materials. *Journal of Engineering Science and Technology*, *15*(6), 4367–4382.

Alzamily, A., Al-Jelawy, H. M., & Jashami, H. (2025). *Finite element simulation of shear stud jointed plain concrete pavement utilizing UHPC link slabs*. Springer International Publishing.

ASTM International. (2010). *Standard test method for bond strength of epoxy-resin systems used with concrete* (ASTM C882/C882M).

ASTM International. (2016). *Standard practice for making and curing concrete test specimens in the laboratory* (ASTM C192/C192M).

ASTM International. (2020). *Standard test method for compressive strength of hydraulic cement mortars* (ASTM C109/C109M).

Büyüköztürk, O., & Lau, D. (2002). High performance concrete: Fundamentals and application. *In Proceedings of the International Conference on New Developments in Concrete Technologies* (pp. 177–198).

Consoli, N. C., Rosa, A. D., & Saldanha, R. B. (2013). Crack-healing investigation in bituminous materials. *Journal of Materials in Civil Engineering*, *25*(7), 864–870.

Daneshvar, D., Behnood, A., & Robisson, A. (2022). Interfacial bond in concrete-to-concrete composites: A review. *Construction and Building Materials*, *359*, 129195.

Diab, A. M., Abd Elmoaty, M. A. E., & Tag Eldin, M. R. (2017). Slant shear bond strength between self compacting concrete and old concrete. *Construction and Building Materials*, *130*, 73–82.

Ding, J., Zhu, J., & Kang, J. (2022). Bonding properties and mechanism of the interface between precast UHPC and

post-cast UHPC. *Structures*, *43*, 822–833.
Farouk, A. I. B., & Zhu, J. (2022). Prediction of interface bond strength between ultra-high-performance concrete (UHPC) and normal strength concrete (NSC) using a machine learning approach. *Arabian Journal for Science and Engineering*, *47*(4), 5337–5363.
Feng, S., Xiao, H., & Li, H. (2020). Comparative studies of the effect of ultrahigh-performance concrete and normal concrete as repair materials on interfacial bond properties and microstructure. *Engineering Structures*, *222*, 111122.
Graybeal, B. A. (2006). *Material property characterization of ultra-high performance concrete* (FHWA-HRT-06-103). Federal Highway Administration.
Hu, B., Li, Y., & Liu, L. (2020). Dynamic slant shear bond behavior between new and old concrete. *Construction and Building Materials*, *238*.
Kinaine, A. F., & Al-Jelawy, H. M. (2023). Using short ultra-high performance concrete link slab as an alternative to steel dowel bars in rigid pavements. *IOP Conference Series: Earth and Environmental Science*, *1232*(1).
Liu, B., Zhang, J., Li, X., & Hao, T. (2023). Experimental study on bond performance of steel strands. *Journal of Architecture and Civil Engineering*, *40*(6), 91–100.
Liu, J., Chen, Z., Guan, D., Lin, Z., & Guo, Z. (2020). Experimental study on interfacial shear behaviour between ultra-high performance concrete and normal strength concrete in precast composite members. *Construction and Building Materials*, *261*, 120008.
Momayez, A., Ehsani, M. R., Ramezanianpour, A. A., & Rajaie, H. (2005). Comparison of methods for evaluating bond strength between concrete substrate and repair materials. *Cement and Concrete Research*, *35*(4), 748–757.
Pulkit, K., Saini, B., & Chalak, H. D. (2023). The influence of interfacial bond between substrate and overlay concrete by bi-surface shear test and split prism test. *Technical Journal*, *150*(l), 1–10.
Santos, D. S., Santos, P. M. D., & Dias-Da-Costa, D. (2012). Effect of surface preparation and bonding agent on the concrete-to-concrete interface strength. *Construction and Building Materials*, *37*, 102–110.
Sohail, M. G., Wang, B., Jain, A., Kahraman, R., Ozerkan, N. G., Gencturk, B., Dawood, M., & Belarbi, A. (2018). Advancements in concrete mix designs: High-performance and ultrahigh-performance concretes from 1970 to 2016. *Journal of Materials in Civil Engineering*, *30*(3).
Sun, Q., Wang, Z., Zhou, M., Li, J., Lu, R., Wang, Y., Liao, X., & Zhao, Y. (2023). The influence of moisture and epoxy bonding agents on interfacial behavior between normal concrete substrate and ultrahigh performance concrete as a repair material. *Advances in Materials Science and Engineering*, *2023*, 1–8.
Tu, T. Y., Chen, Y. Y., & Hwang, C. L. (2006). Properties of HPC with recycled aggregates. *Cement and Concrete Research*, *36*(5), 943–950.
Valikhani, A., Jahromi, A. J., Mantawy, I. M., & Azizinamini, A. (2020). Experimental evaluation of concrete-to-UHPC bond strength with correlation to surface roughness for repair application. *Construction and Building Materials*, *238*.
Zhang, B., Yu, J., Chen, W., Chen, J., Li, H., & Niu, J. (2024). Interface shear failure behavior between normal concrete (NC) and ultra-high performance concrete (UHPC). *International Journal of Concrete Structures and Materials*, *18*(1).
Zhang, Y., Zhu, P., Wang, X., & Wu, J. (2020). Shear properties of the interface between ultra-high performance concrete and normal strength concrete. *Construction and Building Materials*, *248*, 118455.

Author(s) Information

Bushra Husssein Al-Aboudi
University of Al-Qadisiyah, Al-Diwaniyah
Iraq
Contact Email: *bushrahussein@qu.edu.iq*

Haider M. Al-Jelawy
University of Al-Qadisiyah
Iraq

To cite this article:

Al-Aboudi, B. H., & Al-Jelawy, H. M. (2025). Bond performance of concrete-to-hpc interface for different surface profiles using slant and bi-surface shear test. *The Eurasia Proceedings of Science, Technology, Engineering and Mathematics (EPSTEM), 37,* 1054-1067.